Interference with KCNJ2 inhibits proliferation, migration and EMT progression of apillary thyroid carcinoma cells by upregulating GNG2 expression

SIYUAN CHEN[1], MIAOMING HUANG[2] and XIARONG HU[1]

[1]The First Department of General Surgery, [2]Department of Otolaryngology, Affiliated Dongguan People's Hospital, Southern Medical University (Dongguan People's Hospital), Dongguan, Guangdong 523059, P.R. China

Received October 10, 2020; Accepted February 15, 2021

DOI: 10.3892/mmr.2021.12261

Abstract. Papillary thyroid carcinoma is a common malignant tumor of the endocrine system. The specific role and molecular mechanism of potassium inwardly rectifying channel subfamily J member 2 (KCNJ2) in papillary thyroid carcinoma remain unknown. In the present study, the underlying mechanism of KCNJ2 in papillary thyroid carcinoma was explored. KCNJ2 expression in thyroid cancer tissues was predicted using the Gene Expression Profiling Interactive Analysis database, and reverse transcription-quantitative PCR and western blot analyses were performed to detect KCNJ2 expression in papillary thyroid carcinoma cell lines. Cell transfection was performed to inhibit KCNJ2 and G protein subunit γ2 (GNG2) expression. In addition, cell proliferation was detected via the colony formation and MTT assays. The wound healing and Transwell assays were performed to assess cell migration and invasion, respectively. Western blot analysis was performed to detect the expression levels of transport-related proteins and interstitial related proteins. The StarBase database was used to detect GNG2 expression in thyroid cancer. The results demonstrated that KCNJ2 expression was upregulated in papillary thyroid carcinoma cells. In addition, interfering with KCNJ2 expression inhibited the proliferation, invasion and migration of papillary thyroid carcinoma cells, and inhibited the epithelial-to-mesenchymal transition (EMT). These processes may be influenced by the upregulation of GNG2 expression induced by KCNJ2 knockdown. Overall , the results of the present study demonstrated that interference with KCNJ2 inhibited proliferation, migration and EMT progression of papillary thyroid carcinoma cells by upregulating GNG2 expression.

Correspondence to: Professor Xiarong Hu, The First Department of General Surgery, Affiliated Dongguan People's Hospital, Southern Medical University (Dongguan People's Hospital), 3 Wan Dao Road South, Dongguan, Guangdong 523059, P.R. China
E-mail: huxiarong2020@163.com

Key words: potassium inwardly rectifying channel subfamily J member 2, papillary thyroid carcinoma, G protein subunit γ2, proliferation, migration, epithelial-to-mesenchymal transition

Introduction

Thyroid cancer is the most common malignant tumor in the endocrine system, among which papillary carcinoma is the most common, accounting for ~88% of thyroid tumors (1). In patients with papillary thyroid carcinoma, the early symptoms are not obvious (2). Thyroid nodules are identified in the majority of patients using B-mode ultrasound during physical examination, and diagnosis is confirmed following histopathological examination (3). Generally, the survival rate of patients without metastasis of papillary thyroid carcinoma is >80% at 10 years following surgical treatment (4). However, in patients with lymph node metastasis, the tumor cannot be completely removed by surgery, thus the prognosis following palliative treatment remains poor (2). Therefore, early detection, diagnosis and surgical treatment are important means to improve the prognosis of patients with papillary thyroid carcinoma.

Traditional chemotherapy drugs generally have no significant effect on thyroid tumors, and surgical treatment is still the preferred treatment for patients with thyroid tumors (5). With the development of molecular biology and immunohistochemical technology in medical diagnosis and auxiliary diagnosis, the application value of molecular markers with high sensitivity and high specificity in auxiliary diagnosis of tumor is gradually increasing. The application of specific molecular markers in tumor screening can indicate early tumor lesions and the presence of lymph node metastasis (6). In addition, targeting and regulating the expression of molecules in cancer can influence the occurrence and development of diseases, thus providing a theoretical basis for targeted therapy in the treatment of cancer.

Potassium channels exist in a variety of cells and are an important determinant of membrane potential (7). By controlling the opening and closing of potassium channels, membrane potential and signal transduction pathways, such as calcium ions, can be changed (8). Previous studies have demonstrated that there are various potassium channels on tumor cells, and these potassium channels play an important role in the regulation of tumor cell proliferation and apoptosis, and their molecular mechanisms are involved in multiple pathways (9-11). In addition, some potassium channels have specific high expression in some tumor cell membranes, which can be used as a basis for novel antitumor targets (12,13).

Potassium inwardly rectifying channel subfamily J member 2 (KCNJ2) gene is located on chromosome 17, 17 q23, its coding protein is inward rectifier potassium channel Kir2.1 (14). The association between KCNJ2 and tumor progression has been demonstrated; however, mechanistic studies have not yet been performed (15). A study has reported that in small cell lung cancer, inhibition of KCNJ2 expression can promote cell apoptosis, inhibit the cell cycle and promote the sensitivity of cancer cells to chemotherapy drugs (16). In addition, silencing KCNJ2 expression can significantly decrease the invasive and metastatic abilities, and epithelial-to-mesenchymal transition (EMT) of gastric cancer cells (17). It has been reported that KCNJ2 expression is upregulated in thyroid cancer tissues (18,19). However, the specific role of KCNJ2 in papillary thyroid carcinoma remains unknown.

Heterotrimeric G protein has been reported to be involved in several biological activities, including cell proliferation, differentiation, invasion and angiogenesis (20,21). G protein γ2 subunit (Gng2/GNG2) is one of the subunits of the Gβγ-dimer, composed of a heterotrimeric G protein with a Gα-subunit (22). Overexpression of GNG2 inhibits metastasis of human malignant melanoma cells (23). Thus, GNG2 may be a molecular target for the prevention and treatment of malignant melanoma metastasis (23).

The present study aimed to investigate the specific role of KCNJ2 in papillary thyroid carcinoma, and its regulatory molecular mechanism to provide a theoretical basis for molecular biological screening and targeted therapy for papillary thyroid carcinoma.

Materials and methods

Cell culture. The papillary thyroid carcinoma cell lines, BCPAP and TPC-1, and the human thyroid normal cell line, Nthy-ori 3-1, were purchased from The Cell Bank of Type Culture Collection of The Chinese Academy of Sciences and maintained in DMEM (Gibco; Thermo Fisher Scientific, Inc.) supplemented with 10% FBS (Gibco; Thermo Fisher Scientific, Inc.) and 1% (v/v) penicillin/streptomycin (Sigma-Aldrich; Merck KGaA) at 37˚C with 5% CO_2.

Bioinformatics analysis. StarBase website (version 2.0, http://starbase.sysu.edu.cn/) was used to predict the expression of KCNJ2 and GNG2 in all types of thyroid cancer (24). The STRING website (version 11.0, https://string-db.org/) was used to predict the relationship between KCNJ2 and GNG2. The expression of KCNJ2 in thyroid cancer tissues was predicted using the GEPIA database (gepia.cancer-pku.cn/) (25).

Reverse transcription-quantitative (RT-q)PCR. Total RNA was extracted from cells using TRIzol® reagent (Invitrogen; Thermo Fisher Scientific, Inc.). Total RNA was reverse transcribed into cDNA at ~65˚C for 10 min using the SuperScript™ III Reverse Transcriptase kit (cat. no. 18080093; Invitrogen; Thermo Fisher Scientific, Inc.) according to the manufacturer's instructions. qPCR was subsequently performed using the SYBR Green qPCR Master mix (Takara Biotechnology Co., Ltd.) and StepOnePlus Real-Time PCR system (Thermo Fisher Scientific, Inc.). The thermocycling conditions were as follows: 95˚C for 10 min, 40 cycles of 95˚C for 10 sec, 55˚C for 10 sec, and 72˚C for 30 sec. KCNJ2 and GNG2 were normalized to the internal reference gene GAPDH. Relative expression levels were calculated using the $2^{-\Delta\Delta Cq}$ method (26). The following primer sequences were used for qPCR: GNG2 forward, 5'-ATCGATATGGCC ACCAACAACACAGCTA-3' and reverse, 5'-TTACAGGAT GGCAGAAGAAC-3'; KCNJ2 forward, 5'-TGGATGCTGGTT ATCTTCTGC-3' and reverse, 5'-AGCCTATGGTTGTCTGGG TCT-3'; and GAPDH forward, 5'-TCAAGGCTGAGAACG GGAAG-3' and reverse, 5'-TGGACTCCACGACGTACTCA-3'.

Western blotting. Total protein was extracted from each group of cells using RIPA lysis buffer (Sigma-Aldrich; Merck KGaA) and the protein concentrations were determined using a BCA protein assay kit (Bio-Rad Laboratories, Inc.). A total of 40 μg protein/well was separated via SDS-PAGE on 10% gel. The separated proteins were subsequently transferred onto polyvinylidene difluoride membranes (Bio-Rad Laboratories, Inc.) and pre-blocked with 5% non-fat milk for 1 h at room temperature. The membranes were then incubated with rabbit anti-human polyclonal antibody and mouse anti-human GAPDH monoclonal antibody (1:1,000; Abcam) overnight at 4˚C. Membranes were washed with PBS and incubated with secondary HRP-conjugated anti-rabbit antibody (1:5,000; cat. no. ab205718; Abcam) for 1 h at room temperature. Protein bands were visualized using an enhanced chemiluminescence detection system (EMD Millipore), and protein band intensity was determined using ImageJ software (version 146; National Institutes of Health). The ratio of gray value of target protein band to that of GAPDH was regarded as the relative protein expression. The following primary antibodies were used: Anti-KCNJ2 (1:1,000; cat. no. ab109750; Abcam), anti-matrix metalloproteinase (MMP)2 (1:1,000; cat. no. ab92536; Abcam), anti-MMP9 (1:1,000; cat. no. ab76003; Abcam), anti-N-cadherin (1:1,000; cat. no. ab76011; Abcam), anti-Snail (1:1,000; cat. no. ab216347; Abcam), anti-zinc finger E-box binding homeobox 1 (ZEB1; 1: 1,000; cat. no. ab203829; Abcam), anti-GNG2 (1:1,000; cat. no. ab198225; Abcam) and anti-GAPDH (1:1,000; cat. no. ab8245; Abcam).

Plasmid construction and transfection. The KCNJ2 gene was knocked down using two different KCNJ2 short hairpin (sh)RNAs (shKCNJ2-1 and shKCNJ2-2) with lentiviral expression vector GV 493. A negative control shRNA (sh-NC) was used to control for off-target and non-specific effects of shRNA treatment at a concentration of 20 nM. All purchased from Shanghai GenePharma Co., Ltd. Transfection was performed using Lipofectamine® 2000 reagent (Invitrogen; Thermo Fisher Scientific, Inc.). TPC-1 cells were seeded in 6-well plates at a density of $1x10^6$ cells/well. Small interfering RNA (si)-GNG2-1, si-GNG2-2 and NC at a concentration of 20 nM, all purchased from Shanghai GenePharma Co., Ltd. The vectors (Shanghai GenePharma Co., Ltd.) were transfected into TPC-1 cells using Lipofectamine 3000 reagent (Invitrogen; Thermo Fisher Scientific, Inc.), according to the manufacturer's instructions. After transfection for 48 h at 37˚C with 5% CO_2, the transfection efficiency was measured via RT-qPCR analysis, and then subsequent assays were performed after 48 h. The following sequences were used: si-GNG2, 5'-ATAGATCTCCGGACT CTAAGATGAAGTT-3' and 5'-ATAGATCTCCGGACTCTA AGATGAAGTT-3'; and si-NC, 5'-GGA UUGAAUCAAGUC AUUC-3' and 5'-GAAUGACUUGAUUCAAUCC-3'. Cells were divided into the following groups: Control, sh-NC, sh-KCNJ2-2, sh-KCNJ2-2 + si-NC and sh-KCNJ2-2 + si-GNG2-2.

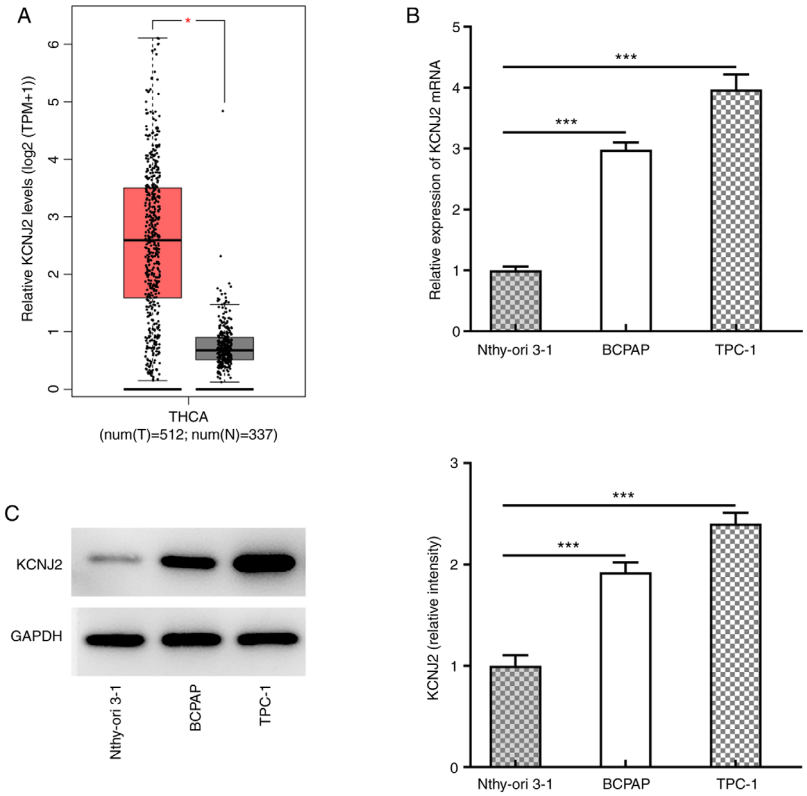

Figure 1. Expression of of KCNJ2 in papillary thyroid carcinoma cells. (A) Gene Expression Profiling Interactive Analysis database prediction results. (B) Reverse transcription-quantitative PCR was performed to detect the mRNA expression of KCNJ2 (n=5). (C) Western blotting was performed to determine the protein expression of KCNJ2 (n=3). *P<0.05, ***P<0.001. KCNJ2, potassium inwardly rectifying channel subfamily J member 2.

MTT assay. The viability of cancer cells was assessed via an MTT assay. Cells ($1x10^3$ cells/well) were seeded into 96-well plates with 0.1 ml for each well and incubated at 37˚C with 5% CO_2. Cells were transfected for 24 h at 37˚C, and 10 μl MTT was subsequently added to each well. Cells were cultivated for an additional 4 h and 150 μl DMSO was added to each well and shaken at low speed for 10 min to make the crystals fully dissolved. Viability was subsequently analyzed at a wavelength of 570 nm, using the Fisherbrand™ accuSkan™ GO UV/Vis microplate spectrophotometer (Thermo Fisher Scientific, Inc.).

Colony formation assay. Following cell transfection, cells were seeded into 6-well plates at a density of 500 cells/well and cultured in DMEM (Invitrogen; Thermo Fisher Scientific, Inc.) supplemented with 10% FBS (Gibco; Thermo Fisher Scientific, Inc.), under normal conditions for 14 days at 37˚C until visible colonies appeared. Cells were fixed with methanol for 15 min at room temperature and subsequently stained with 0.5% crystal violet (Sigma-Aldrich; Merck KGaA) for 30 min at room temperature, prior to observing the cell colonies with a light contrast microscope (Olympus Corporation; magnification, x1).

Wound healing assay. Cells ($1x10^5$ cells/well) were seeded into 6-well plates and cultured (serum-starved) until they reached 80% confluence. Cell monolayers were subsequently wounded (width, 2 mm) using sterile plastic pipette tips and washed with PBS to remove cell debris. The cells were then cultured with fresh DMEM. Cells were observed in five randomly selected fields under a light microscope (magnification, x100) at 0 and 24 h. The distance of cell migration into the wound area was calculated using ImageJ software v1.48u (National Institutes of Health).

Transwell Matrigel assay. Cells in 200 μl serum-free DMEM were plated in the upper chambers of 24-well Transwell plates (Corning, Inc.) with 8-μm pore inserts coated with Matrigel (BD Biosciences), at a concentration of ~$1x10^6$ cells/ml. DMEM (0.5 ml) supplemented with 10% FBS was plated in the lower chambers. For the invasion assay, Transwell membranes were coated with Matrigel (BD Biosciences) at 37˚C for 30 min, according to the manufacturer's instructions. Following incubation for 24 h at 37˚C with 5% CO_2, cells were fixed with paraformaldehyde for 15 min at 25˚C and stained with 0.1% crystal violet for 30 min at room temperature. Cells in the upper chambers were removed using cotton swabs, while stained cells were observed under a light contrast microscope (Olympus Corporation; magnification, x100).

Statistical analysis. Data are presented as the mean ± standard deviation (n≥3). Statistical analyses were performed using SPSS statistical software (version 22.0; IBM Corp.). Comparisons among multiple groups were analyzed using one-way ANOVA followed by Tukey's post hoc test. P<0.05 was considered to indicate a statistically significant difference.

Results

KCNJ2 expression in papillary thyroid carcinoma cells. The prediction results from the GEPIA database demonstrated that KCNJ2 expression was upregulated in thyroid cancer tissues (Fig. 1A). KCNJ2 expression in papillary thyroid carcinoma

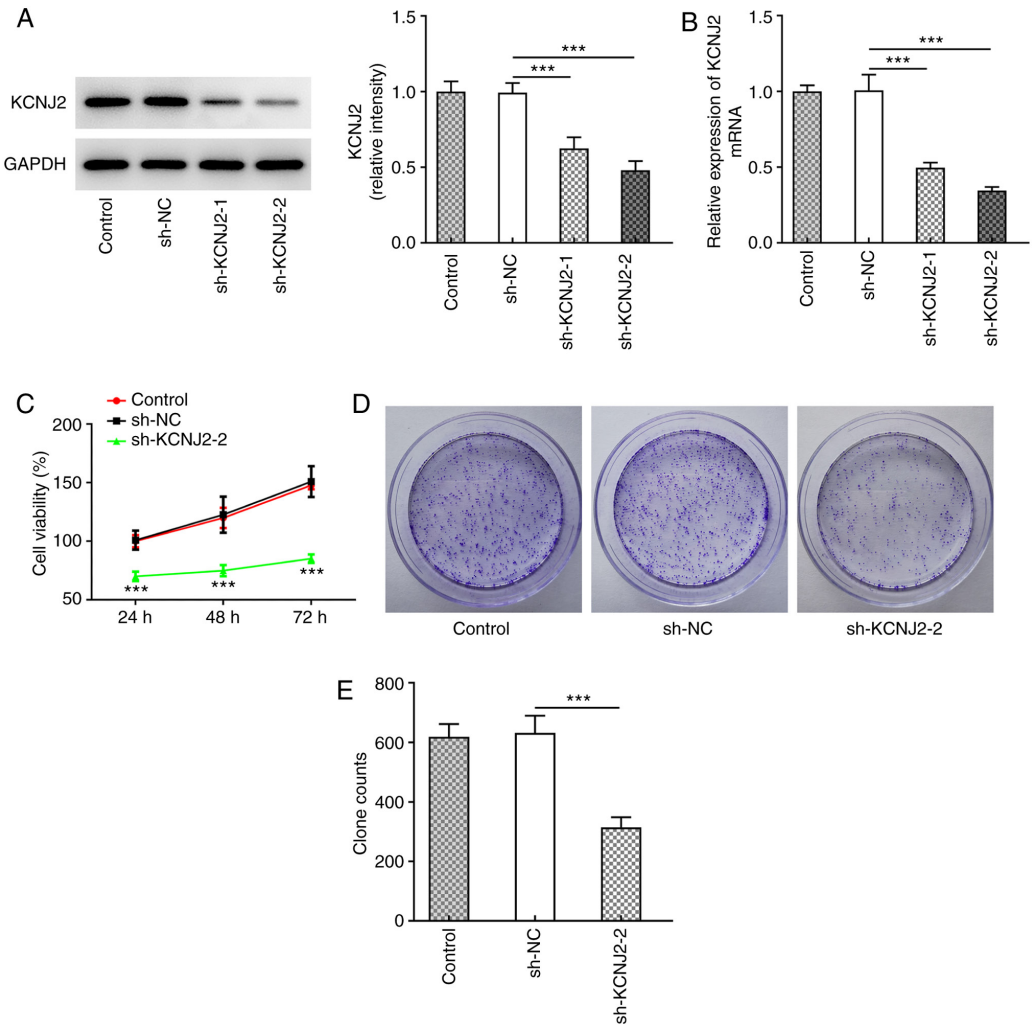

Figure 2. Interfering with KCNJ2 inhibits the proliferation of papillary thyroid carcinoma cells. (A) Western blotting was performed to detect the protein expression of KCNJ2 after cell transfection (n=3). (B) Reverse transcription-quantitative PCR was performed to determine the mRNA expression of KCNJ2 after cell transfection (n=5). (C) An MTT assay was conducted to measure cell proliferation (n=5). (D) A colony formation assay was performed to detect cell proliferation (n=3). (E) Statistical analysis of the results presented in D. ***P<0.001 vs. sh-NC group. KCNJ2, potassium inwardly rectifying channel subfamily J member 2; sh-, short hairpin RNA; NC, negative control.

cell lines was subsequently analyzed. RT-qPCR (Fig. 1B) and western blot analyses (Fig. 1C) demonstrated that KCNJ2 expression was significantly increased in papillary thyroid carcinoma cell lines, with the most significant increase in TPC-1 cells. Thus, TPC-1 cells were selected for subsequent experimentation.

Interfering with KCNJ2 inhibits the proliferation of papillary thyroid carcinoma cells. KCNJ2 expression in papillary thyroid carcinoma cells was inhibited following cell transfection, as assessed via western blotting (Fig. 2A) and RT-qPCR (Fig. 2B). The results demonstrated that KCNJ2 expression was significantly decreased in the sh-KCNJ2-1 and SH-KCNJ2-2 groups compared with the sh-NC group, and the decrease was more notable in the sh-KCNJ2-2 group. Thus, the sh-KCNJ2-2 group was selected for subsequent experimentation. Cell viability was assessed via the MTT (Fig. 2C) and colony formation (Fig. 2D and E) assays. The results demonstrated that the cell survival rate and proliferative ability of cells in the sh-KCNJ2-2 group significantly decreased compared with the sh-NC group. Taken together, these results suggested that interfering with KCNJ2 inhibited the proliferation of papillary thyroid carcinoma cells.

Interfering with KCNJ2 inhibits invasion, migration and the EMT process of papillary thyroid carcinoma cells. The invasive and migratory abilities of papillary thyroid carcinoma cells were assessed. The results of the wound healing assay demonstrated that KCNJ2 knockdown significantly inhibited the migratory ability of papillary thyroid carcinoma cells (Fig. 3A and B). In addition, the results of the Transwell assay demonstrated that KCNJ2 knockdown significantly inhibited the invasive ability of papillary thyroid carcinoma cells (Fig. 3C and D). Western blot analysis was performed to detect the expression levels of the transport-related proteins, MMP2 and MMP9. The results demonstrated that MMP2 and MMP9 expression significantly decreased in the sh-KCNJ2-2 group compared with the sh-NC group (Fig. 3E). The expression levels of the EMT-related proteins, N-cadherin, Snail and ZEB1 were also detected. The results demonstrated that N-cadherin, Snail and ZEB1 expression significantly decreased in sh-KCNJ2-2 group compared with the sh-NC group (Fig. 4).

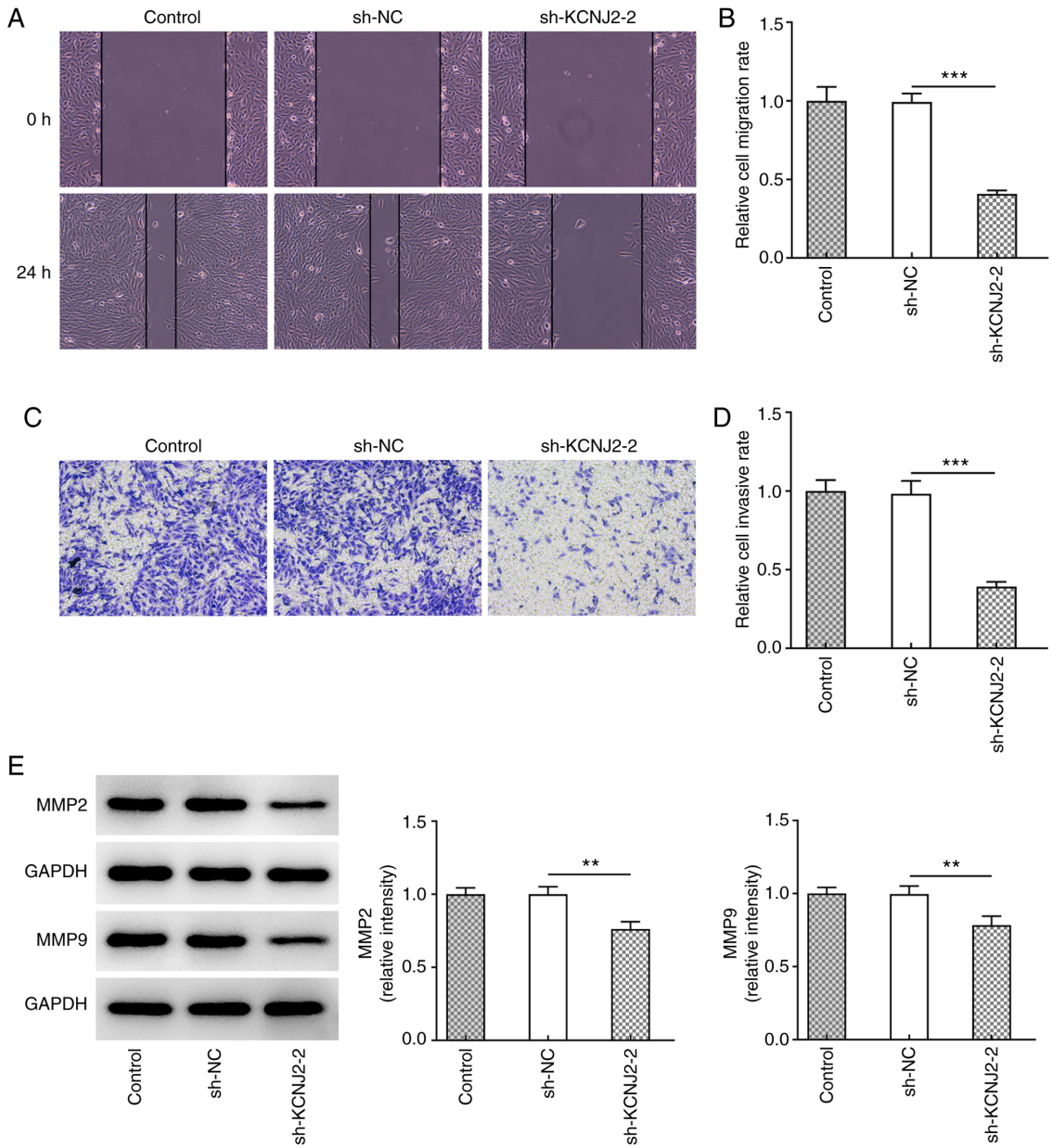

Figure 3. Interfering with KCNJ2 inhibits the migration and invasion of papillary thyroid carcinoma cells. (A) A wound healing assay was performed to measure cell migration (magnification, x100). (B) Statistical analysis of the results presented in A. (C) A Transwell assay was conducted to measure cell invasion (magnification, x100). (D) Statistical analysis of the results presented in C. (E) Western blotting was performed to detect the expression of MMP2 and MMP9. **P<0.01, ***P<0.001. KCNJ2, potassium inwardly rectifying channel subfamily J member 2; sh-, short hairpin RNA; NC, negative control; MMP, matrix metalloproteinase.

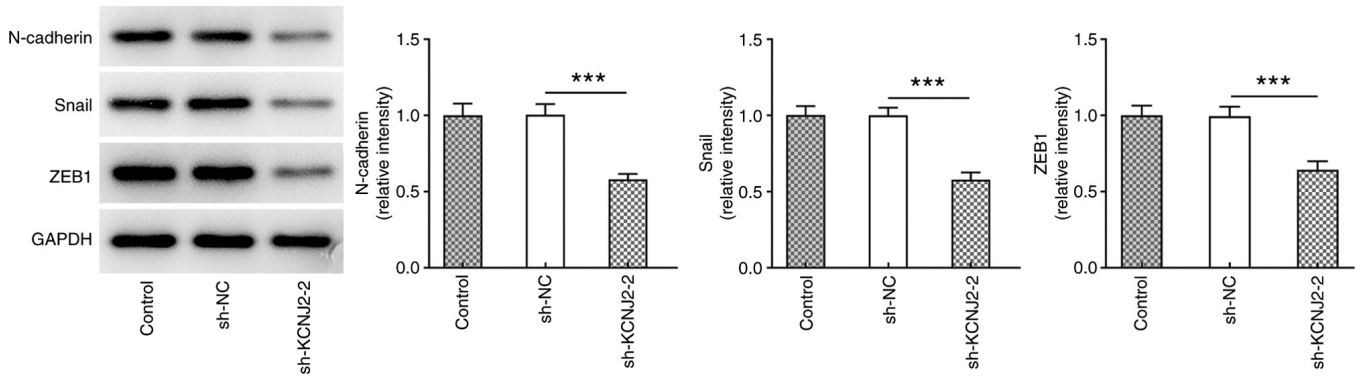

Figure 4. Interfering with KCNJ2 inhibits the EMT of papillary thyroid carcinoma cells. Western blotting was performed to measure the expression of EMT-related proteins (n=3). ***P<0.001. KCNJ2, potassium inwardly rectifying channel subfamily J member 2; sh-, short hairpin RNA; NC, negative control; EMT, epithelial-to-mesenchymal transition; ZEB1, zinc finger E-box binding homeobox 1.

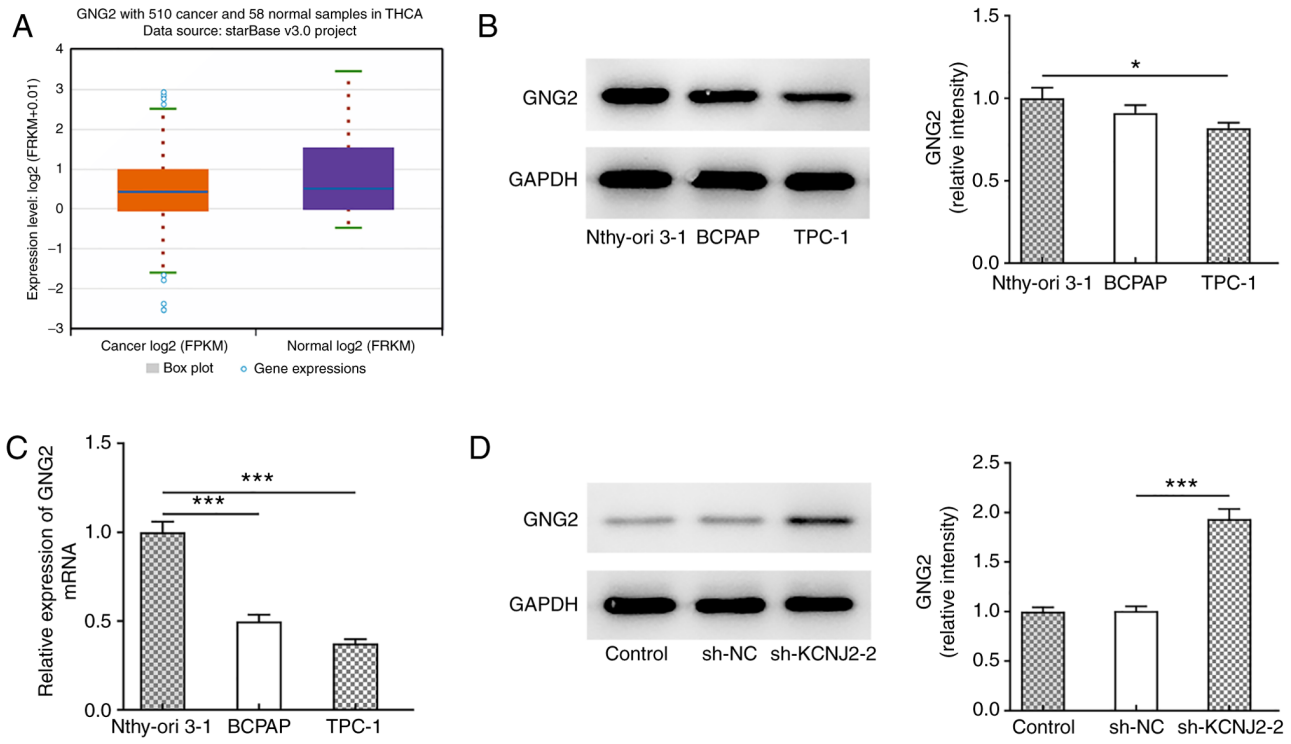

Figure 5. Interfering with KCNJ2 upregulates the expression of GNG2 in papillary thyroid carcinoma cells. (A) Prediction results from StarBase. (B) Western blotting was performed to detect the protein expression of GNG2 (n=3). (C) Reverse transcription-quantitative PCR was conducted to detect the mRNA expression of GNG2 (n=5). (D) Western blotting was performed to determine the protein expression of GNG2 after cell transfection (n=3). *P<0.05, ***P<0.001. KCNJ2, potassium inwardly rectifying channel subfamily J member 2; sh-, short hairpin RNA; NC, negative control; GNG2, G protein subunit γ2.

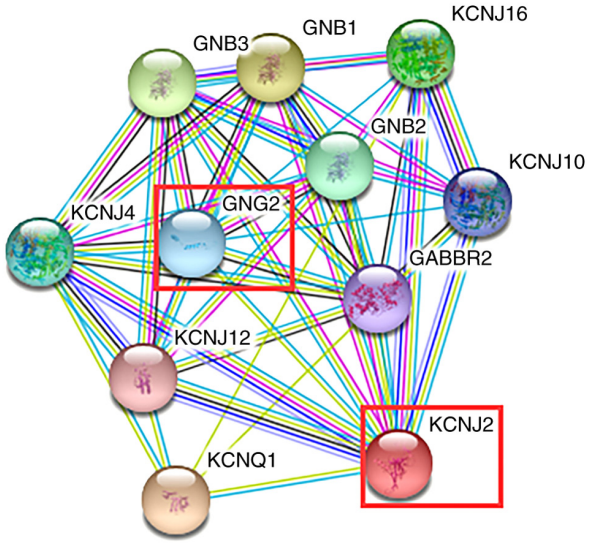

Figure 6. STRING predictions showing the targeted regulatory relationship between KCNJ2 and GNG2. KCNJ2, potassium inwardly rectifying channel subfamily J member 2; GNG2, G protein subunit γ2.

Interfering with KCNJ2 upregulates GNG2 expression in papillary thyroid carcinoma cells. The StarBase database predicted that GNG2 expression was downregulated in thyroid cancer (Fig. 5A), and western blotting (Fig. 5B) and RT-qPCR (Fig. 5C) were performed to detect GNG2 expression in papillary thyroid carcinoma cells. The results demonstrated that GNG2 expression was significantly decreased in papillary thyroid carcinoma cells compared with the normal thyroid cells, Nthy-ori 3-1. Following transfection to suppress KCNJ2 expression, GNG2 expression significantly increased in the sh-KCNJ2-2 group compared with the sh-NC (Fig. 5D). TPC-1 cells were selected for subsequent experimentation. The results from the STRING database demonstrated that KCNJ2 could regulate GNG2 expression (Fig. 6). Collectively, these results suggested that interference with KCNJ2 upregulated GNG2 expression.

Knockdown of GNG2 expression partially reverses the effects of KCNJ2 interference on the proliferation, migration and EMT process of papillary thyroid carcinoma cells. Cell transfection was performed to interfere with GNG2 expression in papillary thyroid carcinoma cells, and western blot analysis was performed to detect the interference effect (Fig. 7A). The results demonstrated that si-GNG2-1 and si-GNG2-2 expression levels significantly decreased compared with the si-NC group, and the decrease was more notable in the si-GNG2-2 group, thus si-GNG2-2 was selected for subsequent experimentation. The MTT (Fig. 7B) and colony formation (Fig. 7C and D) assays were performed to detect the proliferative ability of cells. The results demonstrated that cell viability increased in the sh-KCNJ2-2 + si-GNG2-2 group compared with the sh-KCNJ2-2 + si-NC group, suggesting that GNG2 interference could partially reverse the effect of KCNJ2 interference on papillary thyroid carcinoma cell proliferation. In addition, the results of the wound healing assay demonstrated that cell migration significantly increased in the sh-KCNJ2-2 + si-GNG2-2 group compared with the sh-KCNJ2-2 + si-NC (Fig. 8A and B). The results of the

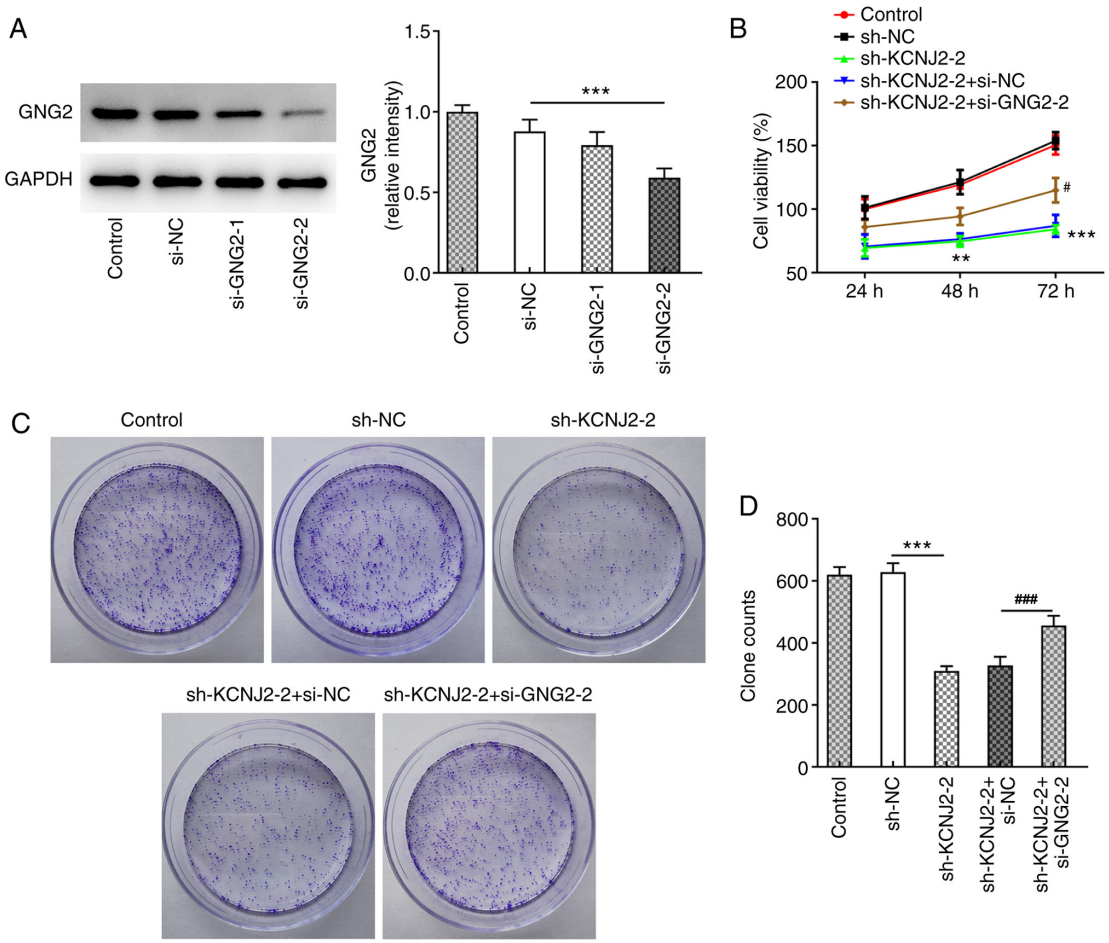

Figure 7. Interference with GNG2 partially reverses the effects of KCNJ2 interference on the proliferation of papillary thyroid carcinoma cells. (A) Western blotting was performed to detect the protein expression of GNG2 after cell transfection (n=3). (B) MTT assay was performed to detect cell viability (n=5). (C) A colony formation assay was conducted to measure cell proliferation (n=3). (D) Statistical analysis of the results presented in C. **P<0.01, ***P<0.001 vs. sh-NC; $^{\#}$P<0.05, $^{\#\#\#}$P<0.001 vs. sh-KCNJ2-2 + si-NC. KCNJ2, potassium inwardly rectifying channel subfamily J member 2; sh-, short hairpin RNA; NC, negative control; GNG2, G protein subunit γ2; si-, small interfering RNA.

Transwell assay demonstrated that cell invasion significantly increased in the sh-KCNJ2-2 + si-GNG2-2 group compared with the sh-KCNJ2-2 + si-NC group (Fig. 8C and D), accompanied by increased MMP2 and MMP9 expression (Fig. 8E). Furthermore, the expression trend of the EMT-related proteins (N-cadherin, Snail and ZEB1) was consistent with that of the migration-related proteins (Fig. 9). Taken together, these results suggested that interference with GNG2 could partially reverse the effects of KCNJ2 interference on papillary thyroid carcinoma cell invasion, migration and the EMT process.

Discussion

According to the GEPIA database, KCNJ2 expression was found to be upregulated in patients with thyroid cancer in the present study. Furthermore, this study also confirmed that KCNJ2 expression was significantly increased in papillary thyroid carcinoma cells, and KCNJ2 knockdown inhibited cell proliferation, invasion, migration and the EMT process. According to the STRING database, there is a regulatory relationship between KCNJ2 and GNG2. In addition, the StarBase database demonstrated that GNG2 expression was downregulated in thyroid cancer. The results of the present study demonstrated that GNG2 expression was significantly downregulated in papillary thyroid carcinoma cells, and GNG2 interference partially reversed the effects of KCNJ2 interference on the proliferation, migration and the EMT process of papillary thyroid carcinoma cells.

The present study demonstrated that KCNJ2 expression was significantly upregulated in TCP-1 papillary thyroid carcinoma cells. This finding was consistent with a previous study by Kim *et al* (18), which reported that KCNJ2 expression is significantly upregulated in papillary thyroid carcinoma tissues compared with normal tissues. KCNJ2 is a potassium ion channel, which plays an important role in the occurrence and development of tumors (27). A previous study demonstrated that KCNJ2 can be used as a biomarker for prognosis of gastric cancer (28). In addition, KCNJ2 can promote the invasion, metastasis and the EMT process of gastric cancer cells by interacting with serine/threonine-protein kinase 38 (17). However, only a few studies have investigated the role of KCNJ2 in other types of cancer and determined its molecular mechanisms (15,29). The results of the present study demonstrated that interference with KCNJ2 expression in papillary thyroid carcinoma

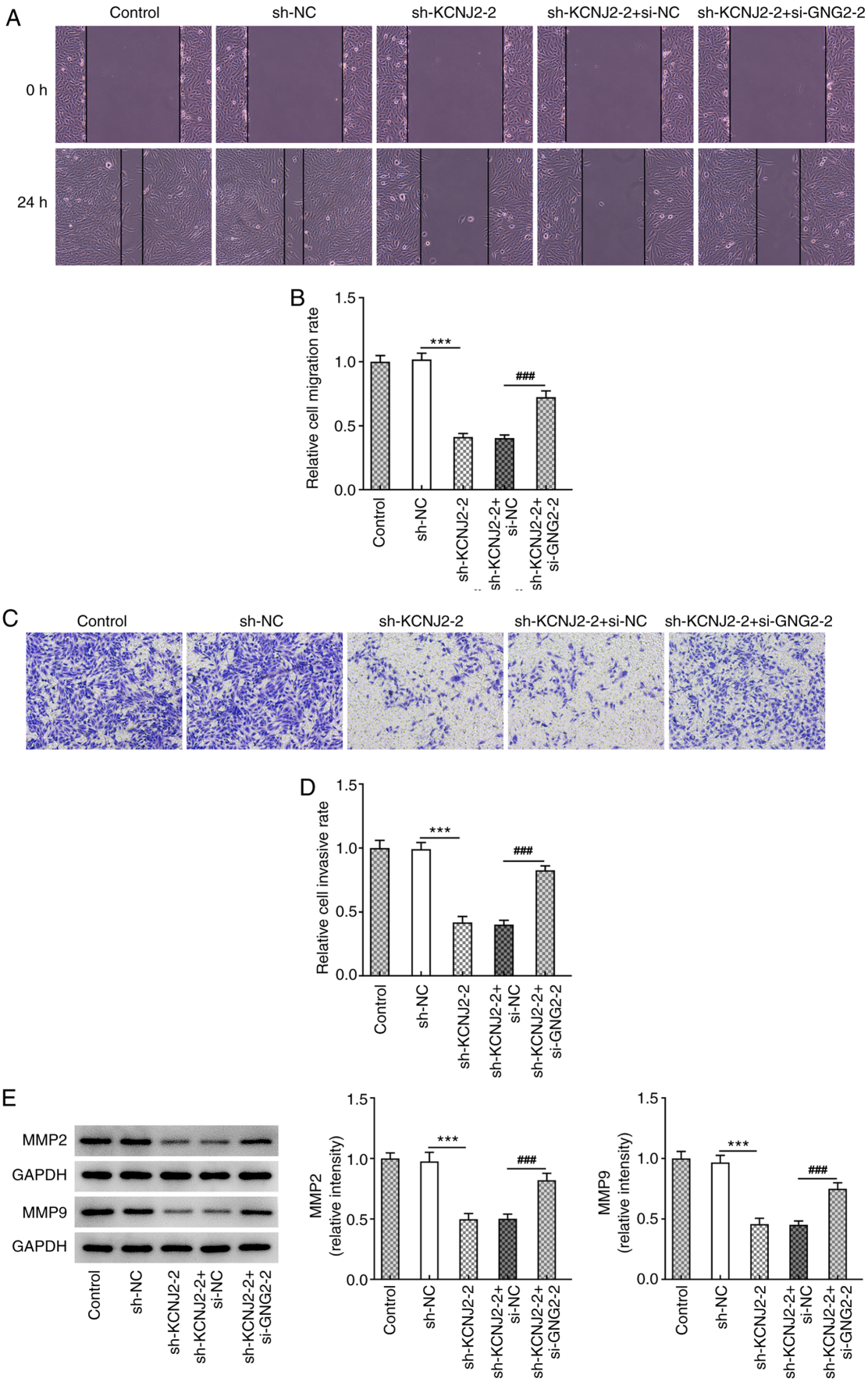

Figure 8. Interference with GNG2 partially reverses the effects of KCNJ2 knockdown on the migration and invasion of papillary thyroid carcinoma cells. (A) A wound healing assay was performed to determine cell migration (magnification, x100). (B) Statistical analysis of the results presented in A. (C) A Transwell assay was performed to detect cell invasion (magnification, x100). (D) Statistical analysis of the results presented in C. (E) Western blotting was performed to measure the expression of MMP2 and MMP9 (n=3). ***P<0.001. $^{###}$P<0.001. KCNJ2, potassium inwardly rectifying channel subfamily J member 2; sh-, short hairpin RNA; NC, negative control; GNG2, G protein subunit γ2; si-, small interfering RNA; MMP, matrix metalloproteinase.

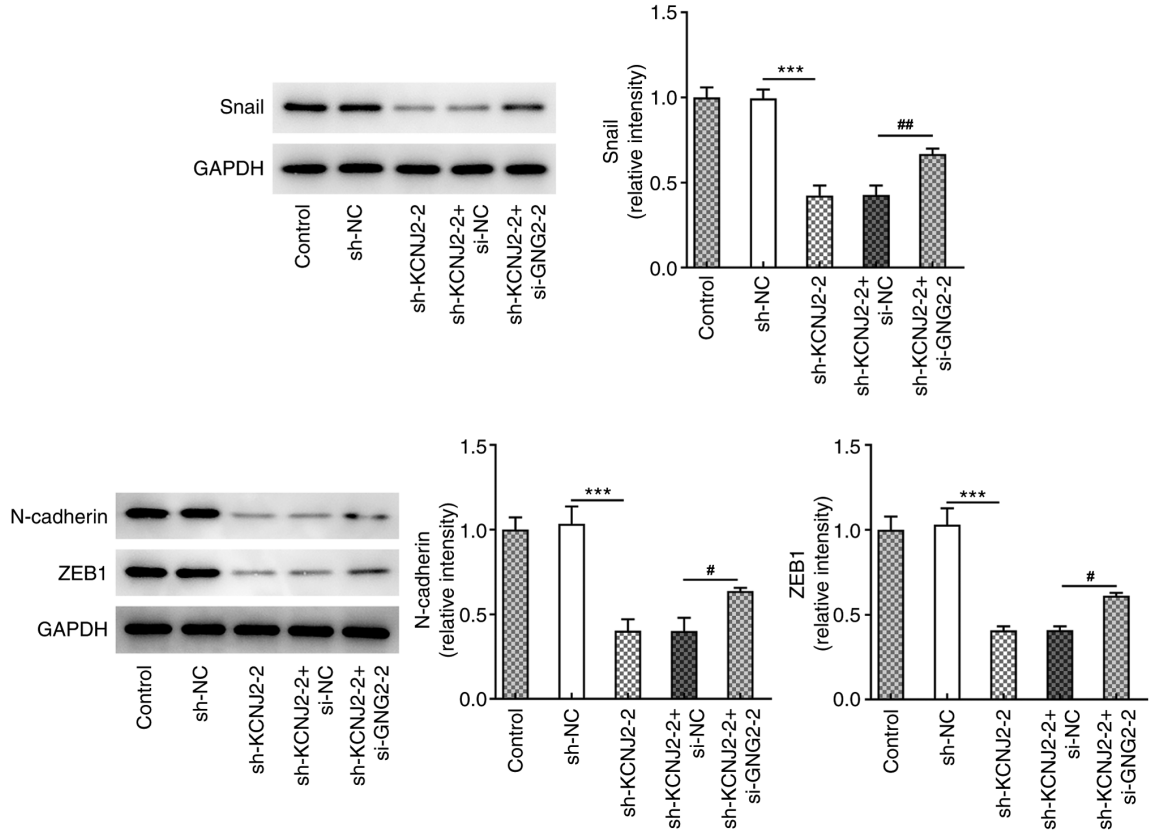

Figure 9. Interference with GNG2 partially reverses the effects of KCNJ2 knockdown on the EMT process of papillary thyroid carcinoma cells. Western blotting was performed to detect the expression of EMT-related proteins (n=3). ***P<0.001. #P<0.05, ##P<0.01. KCNJ2, potassium inwardly rectifying channel subfamily J member 2; sh-, short hairpin RNA; NC, negative control; GNG2, G protein subunit γ2; si-, small interfering RNA; EMT, epithelial-to-mesenchymal transition; ZEB1, zinc finger E-box binding homeobox 1.

cells significantly decreased the proliferative, invasive and migratory abilities of the cells, and inhibited the EMT process. Of note, the BCPAP thyroid cancer cells used in the present study have been proven to be a problematic cell line as they are considered to be poorly differentiated thyroid cancer cells (30). However, these effects did not have any impact on the experimental results of the present study, as it was confirmed that KCNJ2 was expressed at low levels in TPC-1 papillary thyroid carcinoma cells, as predicted by the GEPIA database. Thus, all experiments were performed using TPC-1 cells.

Previous studies on GNG2 focus on its role in melanoma, for example a previous study demonstrated that GNG2 expression is downregulated in mouse malignant melanoma and human melanoma cell lines (31). Overexpression of GNG2 enhances the proliferation of melanoma cells, suggesting that GNG2 may be a novel molecular target for the treatment of malignant melanoma (32). The results of the present study demonstrated that GNG2 expression was downregulated in papillary thyroid carcinoma cells; however, its specific molecular mechanism has not yet been investigated. Prediction analysis revealed that KCNJ2 can combine to regulate GNG2. Following interference with KCNJ2 expression, GNG2 expression significantly increased in papillary thyroid carcinoma cells, suggesting that KCNJ2 may regulate GNG2 expression in papillary thyroid carcinoma. In addition, the results confirmed that GNG2 interference could partially reverse the effects of KCNJ2 interference on the proliferation, migration and the EMT process of papillary thyroid carcinoma cells.

In conclusion, the results of the present study demonstrated the role of KCNJ2 in papillary thyroid carcinoma and discussed its molecular mechanism, providing a theoretical basis for molecular targeted therapy of papillary thyroid carcinoma.

Acknowledgements

Not applicable.

Funding

No funding was received.

Availability of data and materials

The datasets used and/or analyzed generated during the current study are available from the corresponding author on reasonable request.

Authors' contributions

XH wrote the manuscript and analyzed the data. SC and MH performed the experiments and literature search, supervised

the present study and revised the manuscript. XH and SC confirm the authenticity of all the raw data. All authors read and approved the final manuscript.

Ethics approval and consent to participate

Not applicable.

Patient consent for publication

Not applicable.

Competing interests

The authors declare that they have no competing interests.

References

1. Howitt BE, Chang S, Eszlinger M, Paschke R, Drage MG, Krane JF and Barletta JA: Fine-needle aspiration diagnoses of noninvasive follicular variant of papillary thyroid carcinoma. Am J Clin Pathol 144: 850-857, 2015.
2. Lewinski A and Adamczewski Z: Papillary thyroid carcinoma: A cancer with an extremely diverse genetic background and prognosis. Pol Arch Intern Med 127: 388-389, 2017.
3. Ambrosi F, Righi A, Ricci C, Erickson LA, Lloyd RV and Asioli S: Hobnail variant of papillary thyroid carcinoma: A literature review. Endocr Pathol 28: 293-301, 2017.
4. Arianpoor A, Asadi M, Amini E, Ziaeemehr A, Ahmadi Simab S and Zakavi SR: Investigating the prevalence of risk factors of papillary thyroid carcinoma recurrence and disease-free survival after thyroidectomy and central neck dissection in Iranian patients. Acta Chir Belg 120: 173-178, 2020.
5. Tsuchida N, Ikeda MA, Iotashino U, Grieco M and Vecchio G: FUCA1 is induced by wild-type p53 and expressed at different levels in thyroid cancers depending on p53 status. Int J Oncol 50: 2043-2048, 2017.
6. Bogolyubova AV, Abrosimov AY, Selivanova LS and Belousov PV: Histopatological and molecular genetic characteristics of clinically aggressive variants of papillary thyroid carcinoma. Arkh Patol 81: 46-51, 2019.
7. Jackson WF: Potassium channels in regulation of vascular smooth muscle contraction and growth. Adv Pharmacol 78: 89-144, 2017.
8. Martelli A: Potassium channels: A big family, many different targets, great pharmacological opportunities. Curr Med Chem 25: 2626, 2018.
9. Patel SH, Edwards MJ and Ahmad SA: Intracellular ion channels in pancreas cancer. Cell Physiol Biochem 53: 44-51, 2019.
10. Zhang L, Zou W, Zhou SS and Chen DD: Potassium channels and proliferation and migration of breast cancer cells. Sheng Li Xue Bao 61: 15-20, 2009.
11. Zhang P, Yang X, Yin Q, Yi J, Shen W, Zhao L, Zhu Z and Liu J: Inhibition of SK4 potassium channels suppresses cell proliferation, migration and the epithelial-mesenchymal transition in triple-negative breast cancer cells. PLoS One 11: e0154471, 2016.
12. Teisseyre A, Gasiorowska J and Michalak K: Voltage-gated potassium channels Kv1.3-potentially new molecular target in cancer diagnostics and therapy. Adv Clin Exp Med 24: 517-524, 2015.
13. Jiang S, Zhu L, Yang J, Hu L, Gu J, Xing X, Sun Y and Zhang Z: Integrated expression profiling of potassium channels identifys KCNN4 as a prognostic biomarker of pancreatic cancer. Biochem Biophys Res Commun 494: 113-119, 2017.
14. Huang C, Sindic A, Hill CE, Hujer KM, Chan KW, Sassen M, Wu Z, Kurachi Y, Nielsen S, Romero MF and Miller RT: Interaction of the Ca^{2+}-sensing receptor with the inwardly rectifying potassium channels Kir4.1 and Kir4.2 results in inhibition of channel function. Am J Physiol Renal Physiol 292: F1073-F1081, 2007.
15. Franke M, Ibrahim DM, Andrey G, Schwarzer W, Heinrich V, Schopflin R, Kraft K, Kempfer R, Jerković I, Chan WL, *et al*: Formation of new chromatin domains determines pathogenicity of genomic duplications. Nature 538: 265-269, 2016.
16. Liu H, Huang J, Peng J, Wu X, Zhang Y, Zhu W and Guo L: Upregulation of the inwardly rectifying potassium channel Kir2.1 (KCNJ2) modulates multidrug resistance of small-cell lung cancer under the regulation of miR-7 and the Ras/MAPK pathway. Mol Cancer 14: 59, 2015.
17. Ji CD, Wang YX, Xiang DF, Liu Q, Zhou ZH, Qian F, Yang L, Ren Y, Cui W, Xu SL, *et al*: Kir2.1 interaction with Stk38 promotes invasion and metastasis of human gastric cancer by enhancing MEKK2-MEK1/2-ERK1/2 signaling. Cancer Res 78: 3041-3053, 2018.
18. Kim HS, Kim DH, Kim JY, Jeoung NH, Lee IK, Bong JG and Jung ED: Microarray analysis of papillary thyroid cancers in Korean. Korean J Intern Med 25: 399-407, 2010.
19. Oczko-Wojciechowska M, Pfeifer A, Jarzab M, Swierniak M, Rusinek D, Tyszkiewicz T, Kowalska M, Chmielik E, Zembala-Nozynska E, Czarniecka A, *et al*: Impact of the tumor microenvironment on the gene expression profile in papillary thyroid cancer. Pathobiology 87: 143-154, 2020.
20. Leung T, Chen H, Stauffer AM, Giger KE, Sinha S, Horstick EJ, Humbert JE, Hansen CA and Robishaw JD: Zebrafish G protein gamma2 is required for VEGF signaling during angiogenesis. Blood 108: 160-166, 2006.
21. Schwindinger WF and Robishaw JD: Heterotrimeric G-protein betagamma-dimers in growth and differentiation. Oncogene 20: 1653-1660, 2001.
22. Pirone A, Cozzi B, Edelstein L, Peruffo A, Lenzi C, Quilici F, Antonini R and Castagna M: Topography of Gng2- and NetrinG2-expression suggests an insular origin of the human claustrum. PLoS One 7: e44745, 2012.
23. Yajima I, Kumasaka MY, Yamanoshita O, Zou C, Li X, Ohgami N and Kato M: GNG2 inhibits invasion of human malignant melanoma cells with decreased FAK activity. Am J Cancer Res 4: 182-188, 2014.
24. Li JH, Liu S, Zhou H, Qu LH and Yang JH: StarBase v2.0: Decoding miRNA-ceRNA, miRNA-ncRNA and protein-RNA interaction networks from large-scale CLIP-Seq data. Nucleic Acids Res 42 (Database Issue): D92-D97, 2014.
25. Tang Z, Li C, Kang B, Gao G, Li C and Zhang Z: GEPIA: A web server for cancer and normal gene expression profiling and interactive analyses. Nucleic Acids Res 45: W98-W102, 2017.
26. Livak KJ and Schmittgen TD: Analysis of relative gene expression data using real-time quantitative PCR and the 2(-Delta Delta C(T)) method. Methods 25: 402-408, 2001.
27. Handklo-Jamal R, Meisel E, Yakubovich D, Vysochek L, Beinart R, Glikson M, McMullen JR, Dascal N, Nof E and Oz S: Andersen-tawil syndrome is associated with impaired PIP_2 regulation of the potassium channel Kir2.1. Front Pharmacol 11: 672, 2020.
28. Cheng C, Wang Q, Zhu M, Liu K and Zhang Z: Integrated analysis reveals potential long non-coding RNA biomarkers and their potential biological functions for disease free survival in gastric cancer patients. Cancer Cell Int 19: 123, 2019.
29. Yang H, Lin HC, Liu H, Gan D, Jin W, Cui C, Yan Y, Qian Y, Han C and Wang Z: A 6 lncRNA-based risk score system for predicting the recurrence of colon adenocarcinoma patients. Front Oncol 10: 81, 2020.
30. van Staveren WC, Solís DW, Delys L, Duprez L, Andry G, Franc B, Thomas G, Libert F, Dumont JE, Detours V and Maenhaut C: Human thyroid tumor cell lines derived from different tumor types present a common dedifferentiated phenotype. Cancer Res 67: 8113-8120, 2007.
31. Yajima I, Kumasaka MY, Naito Y, Yoshikawa T, Takahashi H, Funasaka Y, Suzuki T and Kato M: Reduced GNG2 expression levels in mouse malignant melanomas and human melanoma cell lines. Am J Cancer Res 2: 322-329, 2012.
32. Yajima I, Kumasaka MY, Tamura H, Ohgami N and Kato M: Functional analysis of GNG2 in human malignant melanoma cells. J Dermatol Sci 68: 172-178, 2012.